Mutational Analysis of Conserved Carboxylate Residues in the Nucleotide Binding Sites of P-Glycoprotein†

Ina L. Urbatsch,‡ Michel Julien,‡ Isabelle Carrier,‡ Marc-Etienne Rousseau, Romain Cayrol, and Philippe Gros*

Department of Biochemistry, McGill University, Montréal, Québec, Canada H3G 1Y6

Received May 18, 2000; Revised Manuscript Received September 6, 2000

ABSTRACT: Mutagenesis was used to investigate the functional role of six pairs of aspartate and glutamate residues (D450/D1093, E482/E1125, E552/E1197, D558/D1203, D592/D1237, and E604/E1249) that are highly conserved in the nucleotide binding sites of P-glycoprotein (Mdr3) and of other ABC transporters. Removal of the charge in E552Q/E1197Q and D558N/D1203N produced proteins with severely impaired biological activity when the proteins were analyzed in yeast cells for cellular resistance to FK506 and restoration of mating in a *ste6*Δ mutant. Mutations at other acidic residues had no apparent effect in the same assays. These four mutants were expressed in *Pichia pastoris*, purified to homogeneity, and biochemically characterized with respect to ATPase activity. Studies with purified proteins showed that mutants D558N and D1203N retained 14 and 30% of the drug-stimulated ATPase activity of wild-type (WT) Mdr3, respectively, and vanadate trapping of 8-azido[α-^{32}P]nucleotide confirmed slower basal and drug-stimulated 8-azido-ATP hydrolysis compared to that for WT Mdr3. The E552Q and E1197Q mutants showed no drug-stimulated ATPase activity. Surprisingly, drugs did stimulate vanadate trapping of 8-azido-[α-^{32}P]nucleotide in E552Q and E1197Q at a level similar to that of WT Mdr3. This suggests that formation of the catalytic transition state can occur in these mutants, and that the bond between the β- and γ-phosphates is hydrolyzed. In addition, photolabeling by 8-azido[α-^{32}P]nucleotide in the presence or absence of drug was also detected in the absence of vanadate in these mutants. These results suggest that steps after the transition state, possibly involved in release of MgADP, are severely impaired in these mutant enzymes.

Multidrug resistance (MDR)[1] in cultured cells in vitro and in tumor cells in vivo is often associated with the overexpression of P-glycoprotein (Pgp) (*1*). Pgp is a plasma membrane protein that functions as an energy-dependent drug efflux pump to reduce the level of intracellular drug accumulation (*1*). Drug transport by Pgp is strictly ATP-dependent and may be mechanistically related to the proposed phospholipid translocase activity of Pgp in normal tissues (*1*−*3*). Pgp is formed by two symmetrical halves with similar sequences, each encoding six transmembrane (TM) domains and one nucleotide binding (NB) site. These NB sites contain characteristic consensus Walker A and B sequence motifs, which have been described in a number of ATP binding proteins and ATPases (*4*). The structural features encoded by each Pgp half (six TM domains and one NB domain) define a large protein superfamily known as the ABC (ATP binding cassette) family of membrane transporters (*5*). In addition to the three rodent (Mdr1, Mdr2, and Mdr3) and two human Pgp isoforms (MDR1 and MDR2) (*6*), some of the best studied ABC transporters include the multidrug resistance-associated protein (MRP) family which transports glutathione and glucuronide adducts (*7*), the CFTR chloride channel in which mutations cause cystic fibrosis in humans (*8*), the bacterial drug resistance protein LmrA (*9*), and the histidine permease (*10*).

The key role of ATP binding and hydrolysis in Pgp-mediated drug transport has been demonstrated in transport studies with membrane vesicles from Pgp positive cells and with purified Pgp reconstituted in liposomes (*1*, *6*). Furthermore, the ATPase activity of Pgp has been shown to be strongly modulated by substrates (drugs) or inhibitors of the protein (e.g., verapamil) (*11*−*14*). In addition, ATP binding and hydrolysis have been shown to occur at both NB sites of Pgp (*15*, *16*), and a mechanistic model of the two sites alternating in catalysis has been proposed (*17*). Finally, single-point mutations at the key lysine residue in the Walker A motif (GCG**K**S) and at the key aspartate in the Walker B motif (ILLL**D**) of each NB site have been shown previously to abolish the ability of Pgp to confer MDR in mammalian (*14*, *18*−*20*) and yeast (*21*) cells, and abrogate ATPase activity as assessed by standard P_i release, and by vanadate-induced trapping of nucleotides (*21*). Although significant structural and functional differences are likely to exist among

† This work was supported by research grants to P.G. from the Medical Research Council (MRC) of Canada. P.G. is an International Research Scholar of the Howard Hughes Medical Institute and is a Career Scientist of the MRC of Canada.

* To whom all correspondence should be addressed: Department of Biochemistry, McGill University, 3655 Drummond, Room 907, Montréal, Québec, Canada H3G 1Y6. Phone: (514) 398-7291. Fax: (514) 398-2603. E-mail: gros@med.mcgill.ca.

‡ These authors have contributed equally to this work.

[1] Abbreviations: ABC, ATP binding cassette; DM, *n*-dodecyl β-D-maltoside; DTT, dithiothreitol; L-PC, L-α-lysophosphatidylcholine; MDR, multidrug resistance; Mdr3, mouse *mdr3* P-glycoprotein; MRP, multidrug resistance-associated protein; *mut*^{s}, methanol utilizing slow; NB site, nucleotide binding site; NB1, N-terminal nucleotide binding site; NB2, C-terminal nucleotide binding site; Pgp, P-glycoprotein; PMSF, phenylmethanesulfonyl fluoride; RT, room temperature; SDS−PAGE, sodium dodecyl sulfate−polyacrylamide gel electrophoresis; TM, transmembrane domain; V_i, orthovanadate; WT, wild-type.

10.1021/bi001128w CCC: $19.00
Published on Web 10/24/2000

different ABC proteins, it has been proposed that the overall structures of the NB sites of ABC proteins and of other proteins containing the Walker A and B signatures are probably very similar (*22*, *23*). Thus, additional key catalytic residues involved in ATP hydrolysis are probably conserved in the NB sites of these proteins as well, and candidates for these residues can be suggested by multiple sequence alignments.

Central to the nucleotide binding site of ABC transporters are the two Walker homology sequences (Walker A and B). The amino acids of the Walker A motif (GCGKS) form the phosphate binding loop, or P loop, which wraps around and provides tight binding for the phosphates of ATP (*4*). The Walker B motif (ILLLD) is involved in the coordination of Mg^{2+}, a mandatory cofactor in the hydrolysis of ATP. In ATPases where a structure is known, such as recA, and the F_1 portion of F_1F_0-ATP synthase, the positions of residues that play key roles in hydrolysis have been determined by both site-directed mutagenesis and biochemical studies (*24*, *25*). For example, a key carboxylate residue includes D144 of recA, or D256 of the β-subunit of F_1-ATPase, which is present at the C-terminus of the Walker B motif β-strand, and is the residue that coordinates Mg^{2+} (*26*−*28*). Also included is E96 of recA, or βE188 of F_1-ATPase, which is found in a loop region following a β-strand between the Walker A and B motifs. This carboxylate is responsible for activating the catalytic water molecule and thus initiating hydrolysis (*29*). In other words, E96 of recA and βE188 of F_1-ATPase are catalytic carboxylates.

Recently, a crystal structure has been determined for an ABC transporter, the nucleotide binding subunit, HisP, of the bacterial histidine permease (*10*). Overall, the structure of the HisP dimer is quite different from that of recA and F_1-ATPase. However, several carboxylates that appear to be structurally and functionally related to the activating carboxylates of F_1 and recA are found in proximity to the ATP molecule, in the ATP binding pocket. In HisP, residue D178 hydrogen bonds a water molecule in proximity to the γ-phosphate of ATP. This water molecule has been proposed to replace Mg^{2+} in the crystal structure (*10*), implying that D178 and its homologue in Pgp (D551/D1196) coordinate Mg^{2+} in the NB site. In addition, the adjacent residue, E179, hydrogen bonds a water molecule, possibly activating it to promote nucleophilic attack and hydrolysis of the γ-phosphate, implying that E179 may be the catalytic carboxylate in histidine permease. However, unlike in recA or F_1-ATPase, the catalytic glutamate E179 is not located between the Walker A and B sequences, but within the extended Walker B motif (*10*). Yoshida et al. have proposed the presence of a catalytic carboxylate in ABC transporters (*29*); as a result, the presence of such a residue in Pgp was investigated.

In the study presented here, we have identified 14 acidic amino acids in the nucleotide binding (NB) sites of Pgp (mouse Mdr3) that are highly conserved in the NB sites of ABC transporters. The importance of these conserved carboxylates was tested by mutagenesis followed by functional analysis in yeast cells and after purification and reconstitution of the enzymes. A cluster of three acidic residues within and adjacent to the Walker B motif are shown to be highly mutation sensitive (D551/D1196, E552/E1197, and D558/D1203), with the negative charge at these positions playing a key role in ATP hydrolysis and ADP release.

EXPERIMENTAL PROCEDURES

Multiple Sequence Alignments and Secondary Structure Predictions. We used the server PredictProtein (http://www.embl.heidelberg.de/predict protein) (*30*) to search the SwissProt database for the closest relatives of the NB1 and NB2 sequences of the mouse Mdr3 protein. Two hundred sixty-nine (NB1) and 321 (NB2) partial or complete sequences corresponding to other ABC transporters were found whose amino acid sequences were more than 30% identical with those of the NB1 and NB2 of Pgp, respectively, a percentage proposed as the threshold for structural similarity (*31*). The program then aligned the sequences of the ABC transporters with the neural network MAXHOM (*32*). These multiple sequence alignments are available as Supporting Information.

mdr3 cDNA Modifications. Mutations in NB1 were created by site-directed mutagenesis using a recombinant PCR approach as described previously (*33*) with a primer TK-5 (5′-GTGCTCATAGTTGCCTACA) and the mutagenic oligos for the D450N, E482Q, and D558N mutations: 5′-CTGTCCGTTGATACTGAC-3′, 5′-CGAATGTTCTGGGCAATCGTGGTG-3′, and 5′-CTTTCTGTATTCAGGGCTG-3′, respectively. A second overlapping *mdr3* cDNA fragment was amplified using primer pairs *Hin*cII (5′-GAAAGCTGTCAACGAAGCC-3′) and primer A (5′-CTGTGTCATGACAAGTTTGAA-3′). The amplification products were purified on gel, mixed, denatured at 94 °C for 2 min, and then incubated at 72 °C for 5 min with Vent DNA polymerase (New England Biolabs) in a reaction mixture without primers to generate hybrid DNA fragments. The hybrid products were then amplified using primers TK-5 and oligoA, and a 552 bp *Nru*I−*Sal*I fragment carrying the mutated segment was purified and used to replace the corresponding fragment in the pVT-*mdr3* construct (*34*) which had served as a template in the PCR. This template contains engineered *Nru*I (position 1346) and *Sal*I sites (position 1908) to facilitate cloning of the mutated cDNA portion. To screen for the desired mutations, individual plasmids were isolated and the nucleotide sequence of the entire 552 bp *Nru*I−*Sal*I fragment was determined. A similar strategy was used to create mutants D592N and E604Q. The mutagenic oligos were 5′-CAATGACGTTAGCATTACG-3′ and 5′-GTCATTGTGCAGCAGCAAGGAAA-3′, respectively, and an overlapping cDNA fragment was amplified with the primer pair *Hin*cII and CK-19 (5′-CATTTCAACCACTCCTG-3′). Here, a 340 bp *Sal*I−*Eco*RI fragment carrying the mutated segment was cloned into the corresponding sites of the pVT-*mdr3* construct. All amplification reactions were performed with Vent DNA polymerase. Mutations in NB2 were created by site-directed mutagenesis using a commercially available kit (Amersham, Arlington Heigths, IL) and single-stranded *mdr3.5* cDNA as a template, as previously described (*21*). These templates contained engineered *Nru*I (position 2724), *Sal*I (position 2480), *Spe*I (position 2914), *Sna*BI (position 3889), and *Age*I sites (position 4199) to facilitate subsequent cloning of the mutated cDNA portions. Mutagenic oligos for the D1093N, E1125Q, D1203, and E1249Q mutations were 5′-CTTTGCCATTTAGAAACAC-3′, 5′-GGCAATGTTCTGCGCAATGCTGCAGTC-3′, 5′-TCAGCTCTGAATACAGAAAG-3′, and 5′-AAGGTCAAGCAGCACGGC-3′, respectively. The nucleotide

sequence of the mutated segments was verified prior to their insertion in the corresponding sites of pVT-*mdr3.5* (*21*).

For the E552Q and E1197Q mutants, the *Mlu*I−*Sal*I cassette and the previously described *Pst*I−*Age*I cassette were used. The mutants were created by site-directed mutagenesis using a standard recombinant PCR method (*33*). The PCR conditions were optimized for each primer set; the annealing temperature was usually between 52 and 56 °C with the $MgCl_2$ concentration within the range of 0.5−2.5 mM. The general cycles were as follows: denaturation (94 °C) for 1 min, annealing for 1 min, and DNA synthesis (72 °C) for 2 min. For E552Q, complementary primers were 5′-GGTGGCCTGGTCCAACAAAAG-3′ (E552Q/r) and 5′-GTTGGACCAGGCCACCTCA-3′ (E552Q/f) with two additional anchor primers, 5′-GACAACATACAAGGA-3′ (L-12/f) and 5′-TCATGACAAGTTTGAA-3′ (OligoA/r). For E1197Q, complementary primers were 5′-TGATGTTGCTTGGTCCAGAAG-3′ (E1197Q/r) and 5′-CTTCTGGACCAAGCAACATC-3′ (E1197Q/f) with two additional anchor primers, 5′-CAGCATCCCACATCATC-3′ (mer9f/f) and 5′-CCTTGATTGGAGACTTG-3′ (pVTBamHI/r).

Testing of Mdr3 Function in Yeast Cells. pVT-*mdr3* plasmids carrying either wild-type or mutant versions of *mdr3* were transformed in the yeast *Saccharomyces cerevisiae* strain JPY201 (*MAT***a***ste6*Δ*ura3*) using a lithium chloride technique (*35*). The biological activity of individual mass populations was tested with respect to their capacity to convey cellular resistance to the fungicidal agent FK506 (50 μg/mL) and to restore mating in the *ste6*Δ sterile yeast as previously described (*36*). Mating efficiency was calculated from the ratio of diploid colonies grown on minimal plates to the total number of haploid JPY201 transformants introduced into the mating assay, and is expressed as the percentage of the mating efficiency of WT *mdr3* transformants. Expression of wild-type and mutant Pgp variants in *S. cerevisiae* membranes was monitored by Western blot analysis of crude plasma membrane preparations, using the monoclonal anti-Pgp antibody C219 (Signet Labs Inc.).

Purification of P-Glycoprotein. For expression and purification of D558N and E552Q, *Afl*II−*Eco*RI cDNA subfragments were excised from pVT-*mdr3* and subcloned into the corresponding sites of pHIL-*mdr3.5*-His_6 as previously described (*21*). In the case of the D1203N and E1197Q mutants, they were introduced into pHIL-*mdr3.5*-His_6 as *Eco*RI−*Sna*BI fragments. pHIL-*mdr3.5*-His_6 carrying either wild-type or mutant versions of *mdr3* as well as the control pHIL-D2 vector were transformed into *Pichia pastoris* strain GS115, according to the manufacturer's instructions (InVitrogen, license number 145457). *His*$^+$ transformants exhibiting successful homologous recombination at the *AOX1* locus were identified as being unable to grow on medium containing methanol (methanol utilizing slow or *mut*^{s}). More than 90% of the *His*$^+$*mut*^{s} transformants that were identified were found to express Pgp, and expression levels of wild-type and mutant Mdr3 variants in these clones were very similar. For large-scale preparations of *P. pastoris* membranes, cultures were induced with methanol and plasma membranes were isolated by centrifugation on discontinuous sucrose density gradients, as previously described (*37*). From a 3 L culture, we routinely obtained between 40 and 50 mg of membrane protein at the 16 to 31% sucrose gradient interface. Solubilization and purification of wild-type and mutant Mdr3 variants on Ni−NTA resin (Qiagen) was essentially as described (*21*) and recently modified (*38*).

Assay of ATPase Activity. For ATPase assays, the 80 mM imidazole eluate from the Ni−NTA resin was incubated with 1% *Escherichia coli* lipids (Avanti, acetone/ether preparation) and 1 mM DTT for 30 min at 20 °C, followed by sonication at 4 °C for 30 s in a bath sonicator (Ultrasonic Inc., Plainview, NY). Omission of DTT resulted in a completely inactive Pgp ATPase. Aliquots of 2−5 μL were added into 50 μL of 50 mM Tris-HCl (pH 8.0), 0.1 mM EGTA, 10 mM Na_2ATP, and 10 mM $MgCl_2$, and the mixture was incubated at 37 °C for the appropriate amount of time, during which the reaction was linear, and ≤10% of the added nucleotide was hydrolyzed. Reactions were stopped by addition of 1 mL of 20 mM ice-cold H_2SO_4, and P_i release was assayed as described previously (*39*). For the determination of kinetic parameters, an excess of 2 mM $MgCl_2$ over MgATP concentrations was used. Drugs were added as dimethyl sulfoxide solutions, and the final solvent concentration in the assay was kept at ≤2% (v/v).

Vanadate Trapping and Photoaffinity Labeling with 8-Azido-[α-^{32}P]ATP. 8-Azido[α-^{32}P]ATP photoaffinity labeling was performed as previously described (*21*) with minor modifications. The 80 mM imidazole eluate containing purified Pgp was incubated with 1% *E. coli* lipids (Avanti, acetone/ether preparation) and 1 mM DTT for 30 min on ice, and reconstituted by dialysis at 4 °C (16 h) against 20 volumes of 50 mM Tris-HCl (pH 7.4), 0.1 mM EGTA, and 1 mM DTT. Proteoliposomes were concentrated by centrifugation for 2 h at 4 °C and 100000*g*, resuspended in the same dialysis buffer, and stored as aliquots at −80 °C. DTT concentrations of ≤1 mM did not interfere with subsequent photolabeling. Proteoliposomes containing wild-type or mutant Mdr3 variants were incubated with 5 μM 8-azido[α-^{32}P]ATP (8.5 Ci/mmol), 3 mM $MgCl_2$, 50 mM Tris-HCl (pH 8.0), and 0.1 mM EGTA, with or without 200 μM vanadate in a total volume of 50 μL at 37 °C for the indicated periods of time. Verapamil or valinomycin (either at 100 μM) was included where indicated. The incubations were started by addition of 8-azido[α-^{32}P]ATP and stopped by transfer on ice. Free label was promptly removed by centrifugation at 200000*g* for 30 min at 4 °C in a TL-100 rotor (Beckman), and proteoliposomes were washed and resuspended in 50 μL of ice-cold 50 mM Tris-HCl (pH 8.0) and 0.1 mM EGTA. Samples were kept on ice and irradiated with UV for 5 min [UVS-II Minerallight (260 nm) placed directly above the samples]. At an 8-azido[α-^{32}P]ATP concentration of 5 μM, hydrolysis and subsequent vanadate-induced trapping of nucleotide are about 20 times slower than at 80 μM 8-azido-[α-^{32}P]ATP, a concentration we previously used in vanadate trapping experiments. This appreciably slower hydrolysis rate allows the demonstration of drug-stimulated 8-azido[α-^{32}P]-ATP hydrolysis and vanadate trapping as described previously (*40*). Upon UV irradiation, up to 10% of the mouse Mdr3 molecules became covalently labeled by 8-azido[α-^{32}P]nucleotide and could be detected by gel electrophoresis (*21*). Orthovanadate solutions (100 mM) were prepared from Na_3VO_4 (Fisher Scientific) at pH 10 as described previously (*41*) and boiled for 2 min before each use to break down polymeric species.

Routine Procedures. Protein concentrations were determined by the bicinchoninic acid method in the presence of

Table 1: Conservation of Acidic Amino Acids in the Nucleotide Binding Sites of Mdr3 and of Other ABC Transporters

NBD1					NBD2				
	D	E	% D + E	no. of sequences aligned[a]		D	E	% D + E	no. of sequences aligned[a]
D366	55	20	58	129	E1009	26	40	46	143
D441	54	50	39	267	D1084	58	59	36	328
D450	**138**	**11**	**56**	**267**	**D1093**	**142**	**15**	**50**	**317**
D453[b]	102	26	48	267	E1096[b]	114	44	50	317
E472	29	39	25	269	E1115	90	59	47	319
E482[c]	**50**	**109**	**59**	**269**	**E1125[c]**	**60**	**146**	**64**	**320**
D494	47	78	46	269	E1139	33	109	44	320
E495	25	93	44	269	E1140	24	112	43	320
D551	**266**	**0**	**100[d]**	266	**D1196**	**317**	**0**	**100[d]**	**317**
E552	**9**	**256**	**100[e]**	**266**	**E1197**	**10**	**306**	**100[e]**	**317**
D558	**260**	**1**	**98[e]**	266	**D1203**	**307**	**0**	**97[e]**	**317**
E562	18	85	39	266	E1207	20	89	34	317
D592	**173**	**12**	**70**	264	**D1237**	**227**	**9**	**74**	**317**
E604	**1**	**151**	**62[f]**	246	**E1249**	**2**	**166**	**54[g]**	**310**

[a] Total number of sequences aligned for each position (because some sequences are only partial, not all sequences can be aligned for each position). [b] Predicted by Yoshida (*26*) to be candidate I for a catalytic carboxylate. [c] Predicted by Yoshida (*26*) to be candidate II for a catalytic carboxylate. [d] Residues of the classical Walker B motifs. Previous substitutions D551N and D1196N revealed completely inactive enzymes. By analogy to other ATPases, these residues are involved in forming a complex with Mg^{2+} of MgATP (*25*). [e] These residues are part of the extended Walker B motif typically found in ABC transporters (*5*). [f] Present in only 246 of the 270 aligned ABC transporters. [g] Present in only 310 of the 321 aligned ABC transporters.

1% SDS using bovine serum albumin as a standard. SDS−PAGE was carried out according to Laemmli (*42*) using the Mini-PROTEAN II gel and Electrotransfer system (Bio-Rad). Samples were dissolved in 5% (w/v) SDS, 25% (v/v) glycerol, 0.125 M Tris-HCl (pH 6.8), 40 mM DTT, and 0.01% pyronin Y for 30 min at 37 °C and separated on 7.5% polyacrylamide gels. For immunodetection of Pgp, the mouse monoclonal antibody C219 (Signet laboratories Inc.) was used with the ECL detection system (Amersham). For autoradiography, SDS gels were stained with Coomassie Blue, dried, and exposed overnight at −80 °C to Kodak BioMax films with intensifying screens.

Materials. 8-Azido[α-^{32}P]ATP (8.5 Ci/mmol) and verapamil were purchased from ICN, while valinomycin and FK506 were from Calbiochem. L-α-Lysophosphatidylcholine and acetone/ether-precipitated *E. coli* lipids were from Avanti Polar Lipids, and general reagent grade chemicals were from Sigma.

RESULTS

Identification of Highly Conserved Carboxylate Residues in Mdr3 and Other ABC Transporters. In this study, we aimed to identify catalytically important acidic amino acids present in each of the two NB sites of the Mdr3 ATPase. For this, we searched the SwissProt database and found 269 and 321 other ABC transporters whose amino acid sequences were more than 30% identical to those of the NB1 and NB2 of Pgp, respectively, a percentage proposed as the threshold for structural similarity (*31*). Table 1 lists the most conserved acidic amino acids (aspartate and glutamate) among these sequences and identifies seven sets of acidic amino acids (bold) with a high degree (≥50%) of conservation in both NB sites (Table 1).

Although there may be significant structural differences among NB sites of ABC transporters, the high degree of primary sequence similarity between HisP and the two NB sites of Pgp (48% similar; *43*) has prompted us to use the recently determined crystal structure of the HisP dimer (*10*) as a model for Pgp. Figure 1 shows an alignment of the amino acid sequences of the two NB sites of Mdr3 and HisP, and the location of α-helices and β-strands based on the HisP structure is also indicated. In the case of Mdr3, the beginning of NB1 and NB2 was assigned as the first residue after TM6 and TM12, respectively; the end of NB2 was the carboxy terminus of Mdr3, and alignment with NB2 defined the end of NB1 (Figure 1). The most conserved acidic amino acids and their location relative to the Walker A and B motifs are shown (Figure 1 and Table 1). The first set, D450 and D1093, is located 21 residues downstream of the Walker A motif and located at the C-terminal end of a β-strand. A second set, E482 and D1125, is found 53 residues downstream of the Walker A motif; these residues have previously been suggested as candidate II for a catalytic carboxylate based on alignments of ABC transporters with the F_1-ATPase (*29*) and also by alignment of the NB sites of CFTR with F_1-ATPase (*44*). Aspartate D551 and D1196, respectively, are part of the well-described Walker B motif and have previously been mutated in our laboratory (*21*). By analogy to other ATPases, these aspartates are suggested to form a complex with Mg^{2+} of MgATP. Two more sets, glutamate E552 and E1197, and aspartate D558 and D1203, respectively, are part of an "extended" Walker B motif typical of ABC transporters (*5*), and both sets of carboxylate residues are completely conserved in all ABC transporters that have been analyzed (Table 1). In addition, in the crystal structure of HisP, a glutamate (E179) is located within 4.3 Å of ATP and has been suggested to position the water molecule for a hydrolytic attack on the γ-phosphate (catalytic carboxylate) (*10*). Glutamates E552 and E1197 appear to map at the homologous position of E179 in HisP. Finally, two more sets of conserved carboxylates, D592 and D1237 and E604 and E1249, are situated 40 and 52 amino acids downstream from the Walker B motifs, respectively (Figure 1).

Effects of NB Site Mutations on Mdr3 Function. Single-point mutations D450N, E482Q, E552Q, D558N, D592N, and E604Q were introduced into the NB1 of Mdr3, and mutations D1093N, E1125Q, E1197Q, D1203N, D1237N, and E1249Q were introduced independently into the NB2.

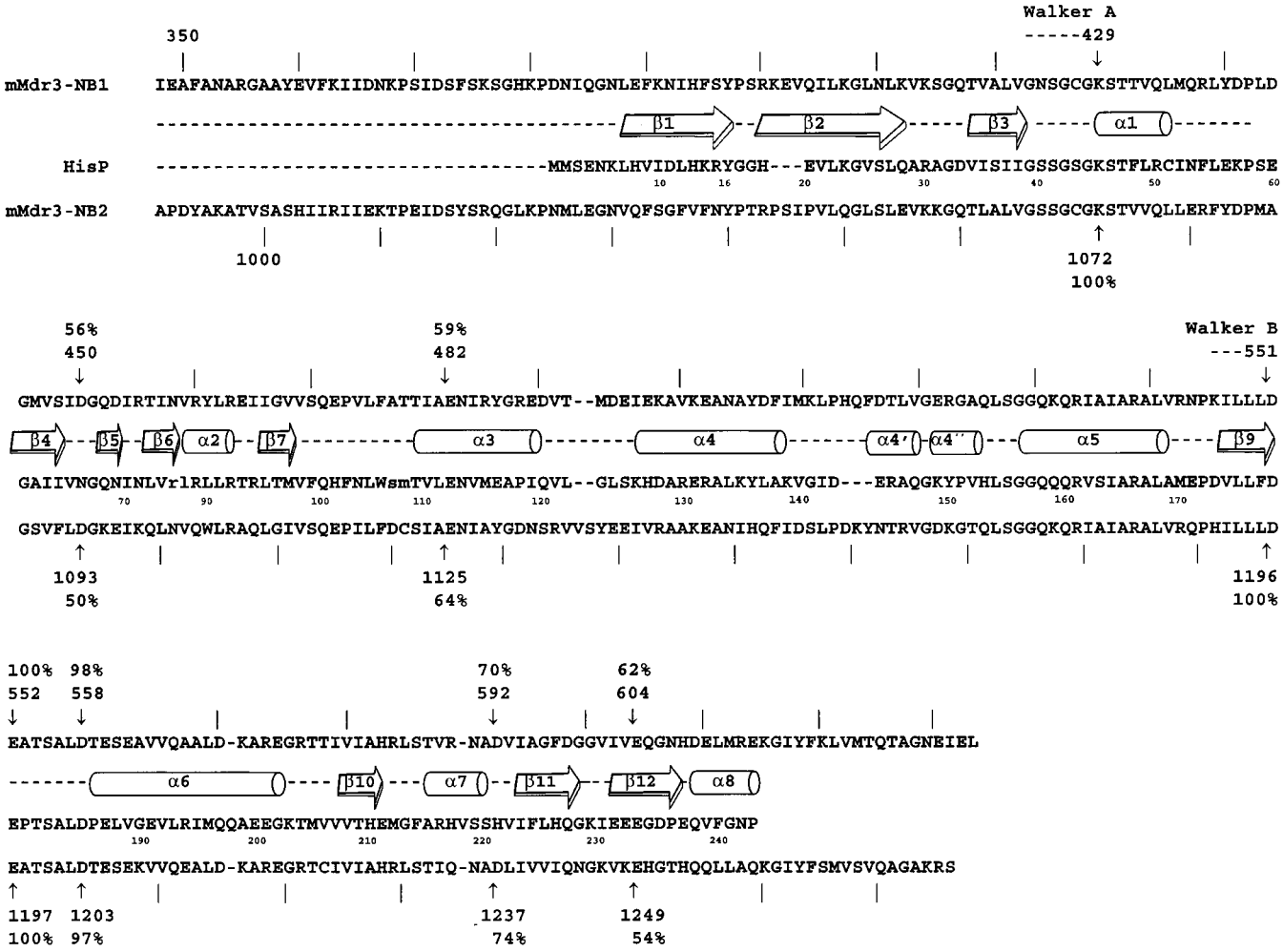

FIGURE 1: Nucleotide binding sites of the mouse Mdr3 ATPase. The amino acid sequences of the N-terminal (NB1) and C-terminal nucleotide binding sites (NB2) of mouse Mdr3 and HisP are aligned (*9*). The beginning of NB1 or NB2 was defined as the first residue after the transmembrane region TM6 or TM12, respectively; the end of NB2 was defined as the carboxy terminus of Mdr3, and alignment with NB2 was used to define the end of NB1. Residues which were ≥50% conserved among ABC transporters (see Table 1) are shown. α-Helices and *β*-strands from the crystal structure of HisP are identified (*9*). Small letters indicate gaps in the HisP sequence.

Mutations were inserted into pVT-*mdr3* and transformed in yeast *S. cerevisiae* strain JPY201. [The Walker B motif mutants D551N and D1196N have previously been shown to abrogate the ability of Mdr3 to confer MDR in vivo, as well as to abolish ATPase activity of the purified enzymes (*21*), and were included here for comparison.] Immunoblotting of crude membrane fractions from yeast transformants expressing individual mutants using the anti-Pgp antibody C219 showed similar levels of expression of the various Pgp mutants (Figure 2), suggesting that these mutations do not have a major effect on Mdr3 stability or membrane targeting in yeast. To assess the biological activity of these mutants, their ability to confer resistance to the fungicide FK506 was tested in a growth inhibition assay in liquid medium (*36*). Cells expressing WT Mdr3 or the NB1 mutants D450N, E482Q, D592N, and E604Q (Figure 3A) or their NB2 counterparts D1093N, E1125Q, D1237N, and E1249Q (Figure 3B) were all resistant to FK506. However, E552Q and D558N (NB1) failed to grow in FK506 and were indistinguishable from negative control *S. cerevisiae* cells transformed with either pVT vector, or with the Walker B motif mutant D551N (Figure 3A). On the other hand, cells expressing D1203N (the NB2 counterpart of the D558N mutant) were also severely impaired for growth in FK506,

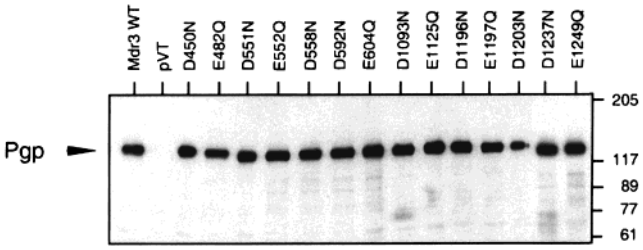

FIGURE 2: Expression of wild-type and mutant Mdr3 variants in *S. cerevisiae*. Western blot analysis of crude plasma membranes from mass populations of individual Mdr3 mutants (identified) in the yeast *S. cerevisiae* using the mouse monoclonal anti-Pgp antibody C219. pVT corresponds to control yeast cells transformed with the plasmid vector. Pgp is identified by an arrow, and the position of molecular mass markers is identified.

although they retained some growth potential which was detectable only upon extended incubation (>26 h) (Figure 3B). In the NB2 group, only mutant E1197Q did not convey resistance to FK506 and showed growth characteristics similar to those of its NB1 counterpart E552Q, the pVT vector control, and the Walker B motif mutant D1196N (Figure 3B). We also measured the capacity of the various Mdr3 mutants to restore mating in the sterile *ste6*Δ yeast strain JPY201 (*36*). The mating frequency was calculated

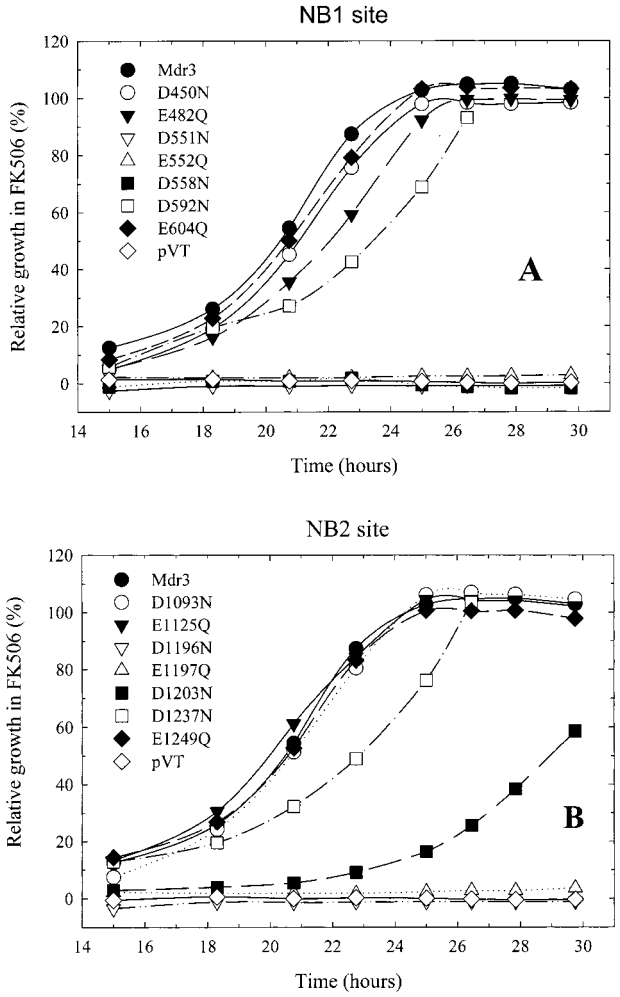

FIGURE 3: Drug resistance of wild-type and mutant Mdr3 variants. The capacity of WT and mutant Mdr3 variants to confer cellular resistance to FK506 in the yeast *S. cerevisiae* was measured by a growth inhibition assay. Growth of individual mass populations in 50 μg/mL FK506 is expressed as the relative growth compared to growth of the same cell populations in drug-free medium (expressed as a percentage). D551N and D1196N are mutations of the classical Walker B motifs previously described (*20*) and were included for comparison. Mutants D551N (▽), E552Q (Δ), and D558N (■) in NB1 (A) and D1196N (▽) and E1197Q (△) in NB2 (B) were indistinguishable from the pVT negative control which does not express Mdr3. Shown is one representative of at least three independent experiments.

as the fraction of transformed JPY201 cells forming diploid colonies on selective medium (over the total number of cells introduced in the assay) and was expressed as a percentage of the mating frequency displayed by WT Mdr3 cells. Mating frequencies of mutants D450N (104%), E482Q (127%), D592N (22%), and E604Q (85%) in NB1 (Figure 4) or their counterparts D1093N (72%), E1125Q (101%), D1237N (68%), and E1249Q (118%) in NB2 (Figure 4) were similar to that of the Mdr3 WT control. However, mating was completely impaired in the NB1 mutants E552Q (<0.1%) and D558N (0.15%), and the frequencies were similar to those measured in the pVT negative control (<0.2%) and for the Walker B mutant D551N (<0.2%) (Figure 4). Mutant E1197Q in the NB2 was completely impaired (<0.1%), similar to its counterpart E552Q in the NB1. In contrast, mutant D1203N in the NB2 (counterpart of D558N) was severely impaired (2.4%), but still retained some residual activity above the background levels seen in pVT or in Walker B motif mutant D1196N (<0.2%) (Figure 4).

Taken together, functional analysis of mutations of the six most conserved carboxylate residues in either NB site identified two sets of carboxylate residues, E552 and E1197 and D558 and D1203, as required for Mdr3 biological activity. These results suggest that these residues play a key role in Pgp function. For further analysis, mutants E552Q and E1197Q as well as D558N and D1203N were expressed in the yeast *P. pastoris* followed by purification and ATPase activity measurements.

Expression and Purification of NB Site Mutants in P. pastoris. For large-scale production of plasma membranes and subsequent Mdr3 purification, we reconstructed E552Q and E1197Q, and D558N and D1203N, in plasmid vector pHIL-*mdr3*-His_6 and expressed the corresponding Pgp variants in the yeast *P. pastoris* (*21*). Crude membrane fractions were prepared from independent colonies of *P. pastoris* transformants and analyzed for Mdr3 protein expression. All Mdr3 mutants could be stably expressed in membrane fractions of *P. pastoris*, and the levels of expression of the mutants were very similar to that seen in cells expressing WT Mdr3 (data not shown). Individual Mdr3 mutants were purified from large-scale plasma membrane preparations by Ni−NTA chromatography as previously described (*21*). All mutant proteins yielded Mdr3 with equal purities and in similar amounts, comparable to those seen for the wild-type protein, as judged by Coomassie Blue-stained SDS gels and Western blot analysis (Figure 5).

ATPase Activity of Mdr3 and NB Site Mutants. Steady-state ATP hydrolysis by the purified proteins was assessed, following reconstitution in *E. coli* lipids, in the absence and presence of different drugs (Table 2). The very low level of ATPase activity of the negative control pHIL-D2 proteoliposomes ranged from 0.05 to 0.10 μmol min^{-1} mg^{-1} (averages from two purifications), was not stimulated by verapamil, valinomycin, or FK506, and was probably caused by low-level contamination from residual plasma membrane ATPases. On the other hand, WT Mdr3 exhibited a basal ATPase activity [0.34 μmol min^{-1} (mg of protein)$^{-1}$] that could be strongly stimulated by verapamil, valinomycin, and FK506 (3.1−12-fold stimulation). Mutants E552Q and E1197Q exhibited very low basal ATPase activity that was similar to that detected in the pHIL-D2 negative control. However, unlike WT Mdr3, the ATPase activity was not stimulated by any of the drugs that were tested (Table 2). Thus, the loss of drug resistance and *ste*6 complementation seen in the E552Q and E1197Q mutants is associated with a complete loss of drug-stimulated ATPase activity (as measured by standard P_i release assays). These results indicate that carboxylates E552 and E1197 are essential for drug-stimulated ATP hydrolysis by Pgp. Since the mutants did not display any drug stimulation of ATP hydrolysis over a range of drug concentrations that were tested (1−200 μM, data not shown), we could not determine the K_M values as a measure for the binding affinities for MgATP. Preliminary data for 8-azido-ATP binding and drug binding to Pgp did not show major differences from WT Mdr3, suggesting proper folding of the purified enzymes (data not shown).

Mutants D558N and D1203N displayed significant drug-stimulated ATPase activity (Table 2). In the mutant D558N, the K_M (MgATP) was 0.66 and 0.79 mM in the presence of

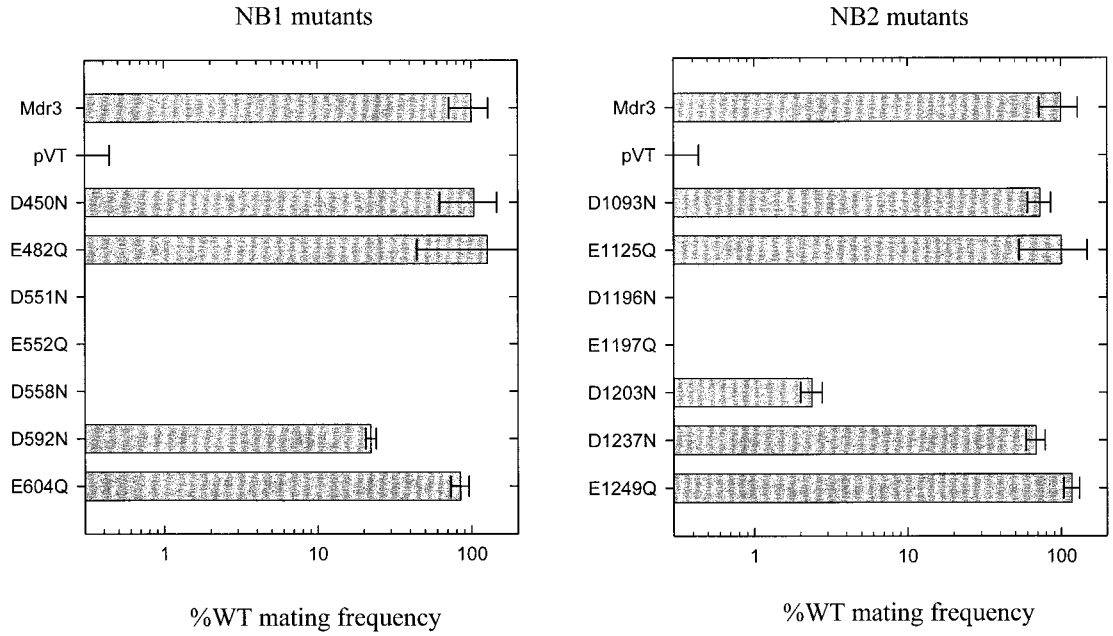

FIGURE 4: Mating frequencies of yeast mass populations expressing wild-type and mutant Mdr3 variants. Mating frequency represents the proportion of transformed **a**-type JPY201 cells that formed diploids upon mating with α-type tester cells DC17, followed by plating on minimal medium. Values are the average of at least three independent experiments and are expressed as percentage of the wild-type frequency ± the standard error of the mean. D551N and D1196N are mutations of the classical Walker B motifs previously characterized (*20*).

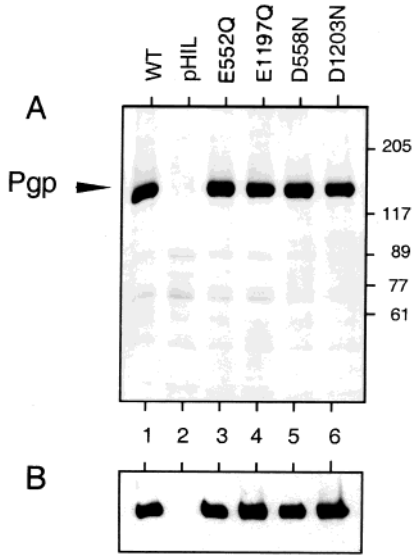

FIGURE 5: Purification of NB site mutants from *P. pastoris* membranes. Wild-type and mutant Mdr3-His_6 variants (identified at the top of panel A) were expressed in the yeast *P. pastoris* and purified by Ni−NTA chromatography. Three micrograms (protein) from the 80 mM imidazole elution fractions was precipitated with TCA, subjected to SDS gel electrophoresis, and stained with Coomassie Blue (A). Western blot analysis of purified proteins with the mouse monoclonal anti-P-glycoprotein antibody C219 (B). The positions of molecular mass markers are given in kilodaltons on the right.

verapamil and valinomycin, respectively, and in the D1203N mutant, the K_M (MgATP) was 0.49, 0.53, and 0.46 mM in the presence of verapamil, valinomycin, and FK506, respectively (the ATPase activity of D558N in FK506 was too low to calculate a K_M accurately). These values were similar to those for WT Mdr3 for all the drugs that were assayed, indicating that the binding affinities for MgATP were not affected. However, V_{max} values varied considerably in these mutant enzymes, and in most cases, there was a good correlation between the activity of these mutants in drug resistance and mating assays and their ATPase activity. In the absence of drug, the ATPase activity of D558N was indistinguishable from that seen in control pHIL-D2 proteoliposomes, and as such was 10 times lower than that for WT Mdr3. However, in the presence of verapamil (100 μM), valinomycin (100 μM), or FK506 (40 μM), this mutant could hydrolyze ATP with a specific activity corresponding to 11, 12, or 18% of WT Mdr3, respectively (Table 2). From this, it appears that an 80−90% reduction in ATPase activity is sufficient to abolish Mdr3 biological activity (in mutant D558N), as assessed by FK506 resistance and *ste6* complementation. The homologous D1203N substitution in the NB2 displayed 26, 29, and 35% of the drug-stimulated ATPase activity of WT Mdr3 (Table 2). Thus, reduced drug resistance and mating activity caused by the D1203N mutation were associated with reduced ATPase activity. Moreover, the more severe effect of the D558N mutation on biological activity (drug resistance) when compared to D1203N was also paralleled by a more severe loss of ATPase activity.

Finally, E552Q, E1197Q, D558N, and D1203N are located just downstream of Walker B motif aspartates D551 and D1196 (Figure 1); thus, we were interested in determining whether these Mdr3 residues may also be involved in forming a complex with Mg^{2+} of MgATP, and whether impaired Mg^{2+} binding may be in part responsible for loss of activity in those mutants. Varying the Mg^{2+} concentration from 0.1 to 100 mM did not restore drug stimulation of ATPase activity in E552Q or E1197Q, and did not increase the drug-stimulated ATPase activity of D558N or D1203N (data not shown). From this, we conclude that both residues are important for efficient ATP hydrolysis to occur in the NB sites of the Mdr3 ATPase, although they are probably not directly involved in complexing Mg^{2+}.

Vanadate Trapping with Mg-8-Azido[α-^{32}P]ATP. We used the technique of vanadate (V_i) trapping of nucleotide to

Table 2: Characteristics of ATPase Activity of Wild-Type Mdr3 and NB Site Mutants

	specific ATPase activity (μmol min^{-1} mg^{-1})[a]			
	no drug	verapamil	valinomycin	FK506
WT	0.34 ± 0.10	3.95 ± 0.10 (12-fold)	3.33 ± 0.33 (10-fold)	1.06 ± 0.073 (3.1-fold)
pHIL-D2[b]	0.066 ± 0.024	0.059 ± 0.004	0.053 ± 0.030	0.097 ± 0.056
E552Q	0.072 ± 0.031	0.077 ± 0.022 (1-fold) (2%[c])	0.084 ± 0.028 (1-fold) (3%)	0.067 ± 0.034 (1-fold) (6%)
E1197Q	0.054 ± 0.026	0.062 ± 0.019 (1-fold) (2%)	0.051 ± 0.022 (1-fold) (2%)	0.059 ± 0.033 (1-fold) (6%)
D558N	0.049 ± 0.044	0.45 ± 0.083 (9.2-fold) (11%)	0.44 ± 0.067 (9.0-fold) (13%)	0.19 ± 0.088 (3.9-fold) (18%)
D1203N	0.093 ± 0.034	1.02 ± 0.146 (11-fold) (26%)	0.95 ± 0.084 (10-fold) (29%)	0.37 ± 0.066 (4.0-fold) (35%)

[a] ATPase activities were assayed as described in Experimental Procedures. All values are the means of at least three experiments ± the standard error of the mean. Values in parentheses are the stimulation over basal activity in the absence of drug. Verapamil, valinomycin, and FK506 were added at concentrations of 100, 100, and 40 μM, respectively. [b] Please note that wild-type and Mdr3 mutants consist of >90% of P-glycoprotein and <10% impurities. Negative control proteoliposomes prepared from vector transformants pHIL-D2 consist of 100% impurities. [c] ATPase activity of individual mutants expressed as a fraction (percentage) of that of wild-type Mdr3.

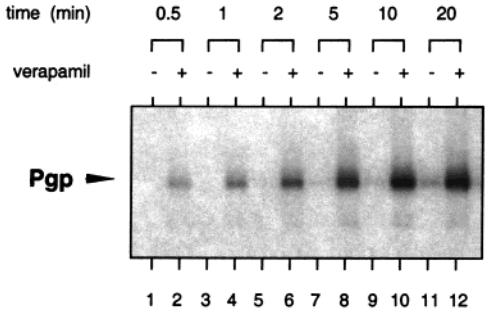

FIGURE 6: Time dependence of vanadate trapping of Mg-8-azido-[α-^{32}P]ATP in wild-type Mdr3. Purified reconstituted wild-type Mdr3 was preincubated with 5 μM 8-azido[α-^{32}P]ATP, 3 mM $MgCl_2$, and 200 μM vanadate in the absence or presence of 100 μM verapamil. The times of preincubation at 37 °C are shown above the lanes. Unbound ligands were removed by ultracentrifugation and washing followed by UV irradiation. Photolabeled samples were separated by electrophoresis on SDS gels and subjected to autoradiography. Experiments were carried out in duplicate.

monitor hydrolysis of Mg-8-azido[α-^{32}P]ATP in each of the NB site mutants of Mdr3. It has been previously established that vanadate trapping requires hydrolysis of ATP and that the trapped nucleotide species in Pgp is ADP (*16*, *46*). The mechanism of vanadate trapping requires first hydrolysis of the bond between the β- and γ-phosphates followed by dissociation of the terminal phosphate (P_i). This allows V_i to come in while MgADP is still bound in the site. V_i then occupies essentially the same position as the γ-phosphate previously did, and a long-lived intermediate is thus formed with bound {Mg·8-azido-ADP·V_i}, which resembles the normal transition state (*16*). In initial experiments, WT Mdr3 was preincubated for 0.5−20 min at 37 °C with 5 μM Mg-8-azido[α-^{32}P]ATP in the presence of vanadate (and in the absence or presence of verapamil) to allow trapping, followed by removal of unbound ligands by centrifugation, and finally cross-linking of the trapped nucleotide by UV irradiation. Photolabeling by the radionucleotide was readily detectable in WT Mdr3 after trapping for only 0.5 min, in the presence of verapamil, and this level of labeling increased rapidly upon augmenting the trapping periods (Figure 6). In the absence of drug, trapping and photolabeling were significantly slower, in agreement with a lower rate of ATP hydrolysis. At an 8-azido[α-^{32}P]ATP concentration of 5 μM, the hydrolysis is slow, allowing one to distinguish between basal and drug-stimulated trapping and photolabeling (*21*, *40*). Under these conditions, vanadate-induced trapping of labeled nucleotide that can be strongly stimulated by verapamil and valinomycin was readily seen in WT Mdr3 (Figure 7A). Trapping and photolabeling were completely absent in control pHIL-D2 proteoliposomes (not shown). As we previously reported (*21*), a mutation at the highly conserved Walker B aspartate of Mdr3 D551 (D551N), which is known to completely impair ATP hydrolysis and drug resistance, also abrogates vanadate-induced trapping of nucleotide in the presence or absence of drugs (Figure 7A).

The purified and reconstituted mutants D558N and D1203N showed basal as well as drug-stimulated trapping and photolabeling in the presence of verapamil or valinomycin (Figure 7B). We overexposed this autoradiograph to show the low level of vanadate-induced trapping of 8-azidonucleotide and photolabeling of the 140 kDa P-glycoprotein in the absence of verapamil or valinomycin (lane 1, Figure 7B), which strongly suggests that the low level of ATP hydrolysis exhibited by D558N (Table 2) is a true reflection of residual Mdr3 ATPase in this mutant, as opposed to contaminating ATPase activities. Increased levels of trapping and photolabeling in the presence of different drugs were noted in the D558N, D1203N, and WT Mdr3 proteins (Figure 7B), in agreement with direct ATP hydrolysis data (Table 2).

Analysis of the E552Q and E1197Q mutants revealed unique and unexpected nucleotide trapping properties. Although E552Q is catalytically inactive in the standard ATPase assay (P_i release), vanadate-induced trapping of 8-azido[α-^{32}P]nucleotide and subsequent photo-cross-linking were seen in E552Q, with trapping strongly stimulated by verapamil and valinomycin (Figure 7A). This drug-stimulated trapping was similar to that detected for WTMdr3, and suggests that this mutant is capable of completing partial reactions of the ATP hydrolysis cycle. An additional unique feature of E552Q is that photolabeling with 8-azido-ATP could also be induced by drug molecules in the absence of vanadate. Under these conditions, the amount of labeled nucleotide bound was smaller than that seen in the presence of vanadate, but was still clearly greater than the very low background levels seen in control conditions lacking vanadate and drugs (Figure 7A). This behavior is clearly distinct from that seen in WT Mdr3, where vanadate is required to observe nucleotide trapping under any condition. The nucleotide trapping properties of the homologous mutant in NBD2, E1197Q, were very similar to those of E552Q with respect to vanadate-induced trapping, and stimulation of trapping by drugs. Interestingly, E1197Q, in addition to being photolabeled in the absence of vanadate and presence of drugs (like E552Q), can also be photolabeled to a low level

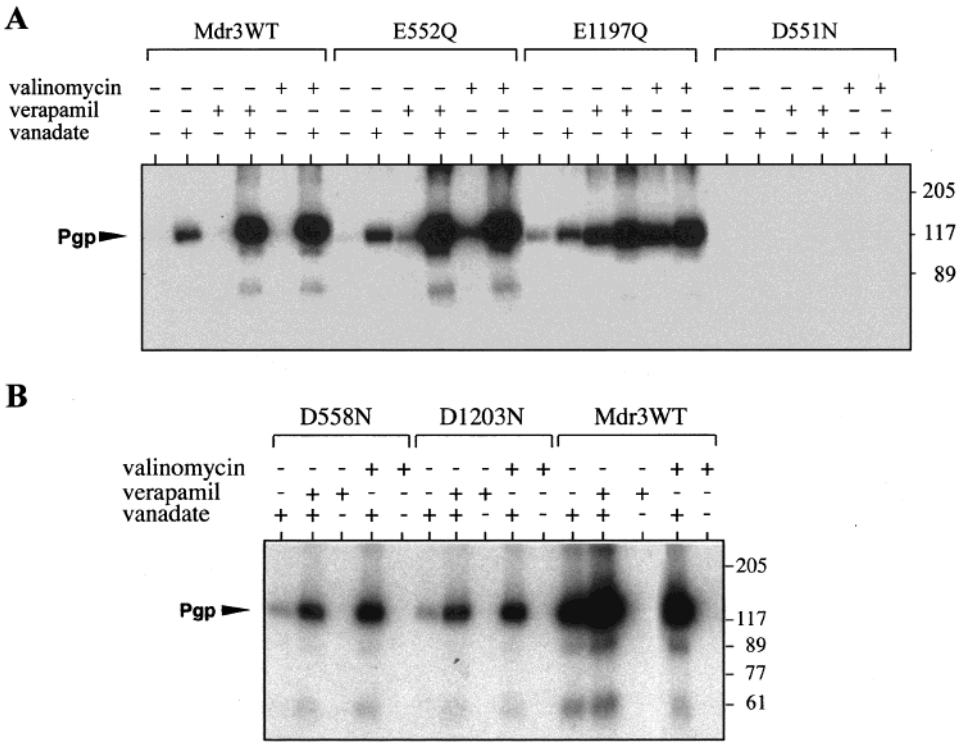

FIGURE 7: Photolabeling of Mdr3 NB site mutants by vanadate trapping with Mg-8-azido[α-^{32}P]ATP. Purified reconstituted wild-type and mutant Mdr3 variants were preincubated with 5 μM 8-azido[α-^{32}P]ATP and 3 mM $MgCl_2$ for 20 min at 37 °C in the absence or presence of 200 μM vanadate. Verapamil (100 μM) or valinomycin (100 μM) was included as indicated above the lanes. Unbound ligands were removed by ultracentrifugation and washing followed by UV irradiation (Experimental Procedures). Photolabeled samples were separated by electrophoresis on SDS gels, transferred to a nitrocellulose membrane, and subjected to autoradiography. Experiments were carried out in duplicate.

in the absence of vanadate and of drug molecules, a behavior distinct from that of E552Q and WT Mdr3. Parallel immunoblotting analysis of the photolabeled WT and mutant Mdr3 indicates equal amounts of protein loaded on gels, and transferred to membrane (data not shown).

DISCUSSION

The aim of the study presented here was to identify catalytically important acidic amino acids in the two NB sites of the Mdr3 ATPase. Sequence alignments of the Mdr3 NB sites with other ABC transporters pointed out seven sets of acidic amino acids which were well conserved (Figure 1). These residues were studied by mutational analysis. Single-point mutations D450N, E482Q, D592N, and E604Q were introduced in NB1 and their homologous substitutions D1093N, E1125Q, D1237N, and E1249Q created in NB2, and the mutants were transformed in the yeast *S. cerevisiae* to assess their biological activity. These four sets of Mdr3 mutants were fully functional in two independent assays, cellular resistance to FK506 (Figure 3), and restoration of mating in an otherwise sterile *ste6*Δ yeast mutant (Figure 4). The results indicate that acidic amino acids at these positions in both NB sites are not critical for Mdr3 transport activity, and thus are unlikely to serve as catalytic carboxylate residues. Several acidic amino acids perfectly conserved among ABC transporters are found in the "extended" Walker B motif which incorporates a highly distinctive signature motif, the consensus HbHbHbHbD (Hb, hydrophobic) followed by "EA/PTSALD" or similar (Figure 1) (*5*). Removal of the charge in D551N and D1196N (previously analyzed in ref *21*), E552Q and E1197Q (this study), and D558N and D1203N (this study) severely impaired transport activity in yeast, and steady-state ATP hydrolysis indicating that these residues are important for Mdr3 function. The negative charge of the glutamate residue at positions 551 and 1196 is completely conserved in the Walker B motif of ABC transporters (Table 1). Mutations at that site have previously been shown to abrogate function by impairing ATPase activity, as measured both in ATPase assays (P_i release) and by vanadate-induced trapping of nucleotides (completion of reaction steps leading to occlusion of $MgADP{\cdot}V_i$) (*21*). While E552Q (NB1), E1197Q (NB2), and D558N (NB1) failed to grow in FK506 (Figure 3) and were completely impaired in mating (Figure 4), D1203N (NB2) retained residual activity in both assays. We purified the mutant enzymes from the yeast *P. pastoris* to monitor Mdr3 specific ATP hydrolysis. Mutants D558N and D1203N both retained readily detectable but low levels of steady-state ATP hydrolysis in the presence of verapamil, valinomycin, and FK506 (Table 2), while mutants E552Q and E1197Q had no drug-stimulated ATPase activity. Thus, the biological activity in yeast seemed to correlate well with the ATPase activity of the purified mutant enzymes. Overall, it appears that a drug-stimulated ATPase activity of ≤18% is insufficient to energize drug transport and show biological activity in yeast; e.g., the biological assay shows sensitivity to impairment of ATPase. Interestingly, a drug-stimulated ATPase activity of 30% in the D1203N mutant supported some biological activity, indicating that interactions may be different for NB1 and NB2, since the mutant at the

homologous residue in the NB1 had more severe effects. Possible functional differences between the NB1 and NB2 of Pgp have recently been documented by Hrycyna et al. (*20*), while studying human MDR1 by photolabeling with 8-azido-ATP under binding and hydrolysis conditions. Finally, an important role for acidic residues in the extended Walker B motifs has been independently noted at the homologous position of distantly related bacterial ABC transporters HisP (*46*), KpsT (*47*), and MalK (*48*).

To further investigate the mechanistic basis for the partial or complete loss of function seen in these mutants, we applied the technique of vanadate trapping of nucleotide in the purified reconstituted NB site mutants. Previous studies have demonstrated that vanadate-induced trapping requires hydrolysis of 8-azido-ATP to 8-azido-ADP and that a stable {Pgp**·Mg·8-azido-ADP·V_i} transition-state complex forms, which can be cross-linked to the protein (*16*, *45*). In the D558N mutant, vanadate trapping and photolabeling of the140 kDa P-glycoprotein band by the 8-azidonucleotide proved that the low level of ATP hydrolysis seen in the absence of drug was clearly associated with the mutant Mdr3 ATPase activity (Figure 7B). Increased levels of trapping and photolabeling in the presence of different drugs in the D558N and D1203N mutants reflected an increased level of MgATP hydrolysis; however, the extent of accumulation of 8-azidonucleotide was much lower in these mutants than in WT Mdr3. The significant but low level of ATP and 8-azido-ATP hydrolysis distinguished both mutants from Walker B motif mutants D551N and D1196N that have no ATPase activity and do not show any vanadate-induced nucleotide trapping in the NB sites (Figure 7A; *21*).

Within different nucleoside triphosphate-hydrolyzing enzymes, the question as to whether a general base residue is essential to the catalytic mechanism of hydrolysis has been a matter of considerable debate. Spatial considerations in the crystal structure of F_1-ATPase suggest that βE188 serves as a general base to activate the water molecule promoting an in-line nucleophilic attack on the γ-phosphate for ATP hydrolysis (*27*). The catalytic power of Mdr3 ($k_{cat} = 10\ s^{-1}$) is 1 order of magnitude lower than that of F_1-ATPase ($k_{cat} = 180\ s^{-1}$). Thus, according to the concept proposed by Mildvan (*49*), the Mdr3 ATPase may rely on a catalytic carboxylate by a mechanism related to F_1-ATPase. Mutants D558N and D1203N still retained 14 and 30% of their drug-stimulated ATPase activity, respectively. This relatively high ATPase activity does not compare with the loss of activity expected for such a catalytic carboxylate in Mdr3. In the crystal structure of HisP, the residue homologous to D558/D1203 is D185. It is located >19 Å away from the γ-phosphate of bound ATP, which is too far away for a direct interaction between the carboxylate of D185 and the γ-phosphate (*10*). Thus, by analogy with F_1-ATPase, it is unlikely to function as a so-called catalytic carboxylate. D185 is located at the interface between β-sheets and the α-helical domain, which has been proposed to interact with the membrane domain, suggesting that D558 and D1203 in Mdr3 might be involved in coupling ATP hydrolysis and drug transport. Alternatively, they might simply be involved in "cross-talk" between the two NB sites to efficiently hydrolyze ATP to energize drug transport.

The parallel analysis of mutants E552Q and E1197Q revealed unique biochemical properties that together provide novel insight into the catalytic cycle of Pgp. Indeed, both mutants share a similar phenotype, which includes a complete loss of steady-state ATP hydrolysis, as assessed by P_i release in a standard assay. However, both mutants show vanadate-induced trapping of nucleotide, which can be strongly stimulated by drugs such as verapamil and valinomycin. Surprisingly, both mutants also exhibit drug-induced labeling by 8-azido-ATP even in the absence of vanadate (Figure 7A). Several observations suggest that the unusual character of these mutants is a true reflection of the loss of negative charge at these positions, as opposed to a nonspecific effect of the mutation on overall three-dimensional structure of the protein, or through other possible artifacts associated with purification or testing procedures. First, this phenotype is very similar for the two mutants. Second, it is associated with a very discrete mutation in the protein, the replacement of a negative charge with an uncharged amino group while retaining a similar size of the residue. Third, an identical mutation at the adjacent residue (D551N and D1196N) has a completely different phenotype, with a loss of both ATP hydrolysis and vanadate-induced nucleotide trapping (Figure 7A). Fourth, both E552Q and E1197Q mutants display drug stimulation of photolabeling by 8-azido-ATP (in the presence or absence of vanadate), suggesting that drug binding and the overall structure of the protein are not grossly affected. Fifth, all mutant and wild-type proteins were purified by the same protocol and tested concurrently and repeatedly with very similar results.

In the presence of vanadate, increased levels of trapping and photolabeling in the E552Q and E1197Q mutants after addition of verapamil or valinomycin were seen and were comparable to WT levels, and reflected formation of the {Pgp**·Mg·8-azido-ADP·V_i} transition-state complex (Figure 7A). The fact that these mutants were deficient in drug-stimulated steady-state ATP hydrolysis, yet fully retained their capability to form the transition-state complex in a drug-dependent manner, suggested that binding of 8-azido-ATP and initiation of hydrolysis leading to formation of the transition-state complex were normal in the E552Q and E1197Q mutant enzymes. However, steps after the formation of the transition state, including release of MgADP and/or P_i, were severely affected. Since the amount of photolabel incorporated in the E552Q and E1197Q mutants under conditions of vanadate alone or vanadate with drug was similar to that detected in the WT protein, it appears unlikely that a major defect in P_i release is present in these mutants. We favor a model in which release of MgADP is severely impaired, and the mutant enzymes are incapable of performing a single complete catalytic cycle. This phenotype is clearly distinct from that of mutants at the adjacent residues in the Walker B motif (D551N and D1196N), which did not show any steady-state ATPase activity and completely lost their capacity to trap 8-azido-ATP with vanadate to form the {Pgp**·Mg·8-azido-ADP·V_i} transition-state complex (*19*, *21*).

Another interesting and distinguishing feature of the E552Q and E1197Q mutant enzymes is the observed drug-induced labeling of the proteins by 8-azidonucleotide in the absence of vanadate, which is clearly absent in the WT Pgp (Figure 7A). We have not yet established whether 8-azido-ATP or 8-azido-ADP (or both) is the nucleotide cross-linked in these mutants under such conditions. Preliminary experi-

ments with direct photolabeling by 8-azido-ATP under binding conditions (4 °C) failed to detect major differences between E552Q, E1197Q, and WT Mdr3 (data not shown), suggesting that the affinity of the mutants for 8-azido-ATP is similar to that of WT Mdr3; in other words, increased affinity for 8-azido-ATP does not seem to be responsible for labeling in the mutant enzymes. It is tempting to speculate that the mutants are capable of cleaving the bond between the β- and γ-phosphates and hence undergo partial reactions toward a full cycle of 8-azido-ATP hydrolysis. However, it remains to be shown whether 8-azido-ADP is the bound nucleotide in the absence of vanadate. If so, MgADP release in these mutants may be sufficiently impaired to provide conditions necessary for cross-linking ADP in the NB sites in the absence of vanadate, a phenomenon not detectable in WT Mdr3 due to rapid turnover of ADP and/or ATP during the normal catalytic cycle. Additionally, it is not known at present in which NB site (or both) of E552Q and E1197Q the nucleotide is occluded. Preliminary trypsin digestion experiments suggest labeling at both NB1 and NB2 in E552Q and E1197Q (data not shown). Finally, the differences in photolabeling of E552Q and E1197Q by the radionucleotide in the absence of vanadate and in the absence or presence of drugs (E1197Q > E552Q) may reflect functional differences between the two NB sites of Pgp. Such differences would not be detected in the presence of vanadate that would stabilize the transition-state complex. Functional differences between the two NB sites of Pgp have been previously noted in photolabeling (*20*) and in trypsin sensitivity experiments (*50*). Additional experiments will be required to further test this hypothesis.

In the crystal structure of HisP, a glutamate (E179) is located within 4.3 Å of the γ-phosphate of bound ATP and forms a hydrogen bond with a water molecule (water 437), which interacts with the γ-phosphate through a hydrogen bond that is nearly parallel to the Pγ−Oβ bond, the bond that breaks upon hydrolysis. Therefore, this residue has been proposed to be the activating residue (catalytic carboxylate) (*10*). Multiple sequence alignments identify E552 and E1197 as Pgp homologues of HisP E179. The loss of drug-stimulated steady-state ATP hydrolysis observed in the E552Q and E1197Q Pgp mutants detected here suggests a similar critical role of these residues in ATP hydrolysis by Pgp. However, substitution of the charged glutamate by its uncharged homologue still allowed formation of the catalytic transition state with bound {Pgp**·Mg·8-azido-ADP·V_i} in the mutant enzymes. This situation is clearly different from that of the catalytic carboxylate mutant βE188Q of F_1-ATPase, where loss of ATPase activity is associated with loss of formation of the catalytic transition state with fluoroaluminate (*51*). Further biochemical and mutational analyses of these residues are warranted, and future crystal structures of ABC transporters in the presence of Mg^{2+} and/or transition-state analogues may give a more precise orientation for the two residues in question, and may provide better insights into this issue.

Together, the identification of two highly mutation-sensitive carboxylate residues at positions 552 and 1197, and 558 and 1203, reported here clearly points at a key functional role for the short helical loop located immediately downstream of the Walker B motif in the catalytic activity of the ATP binding sites of ABC transporters.

ACKNOWLEDGMENT

We thank Drs. Alan Senior and Joachim Weber (University of Rochester, Rochester, NY) for helpful discussions and for critical reading of the manuscript.

SUPPORTING INFORMATION AVAILABLE

Multiple sequence alignments containing 270 sequences for NB1 and 322 sequences for NB2 or their equivalents in ABC transporters. This material is available free of charge via the Internet at http://pubs.acs.org.

REFERENCES

1. Ambudkar, S. V., Dey, S., Hrycyna, C. A., Ramachandra, M., Pastan, I., and Gottesman, M. M. (1999) *Annu. Rev. Pharmacol. Toxicol. 39*, 361−398.
2. Van Helvoort, A., Smith, A. J., Sprong, H., Fritzsche, I., Schinkel, A. H., Borst, P., and van Meer, G. (1996) *Cell 87*, 507−517.
3. Ruetz, S., and Gros, P. (1994) *Cell 77*, 1071−1081.
4. Walker, J. E., Saraste, M., Runswick, M. J., and Gay, N. J. (1982) *EMBO J. 1*, 945−951.
5. Holland, B., and Blight, M. A (1999) *J. Mol. Biol. 293*, 381−399.
6. Gros, P., and Hanna, M. (1996) in *Handbook of Biophysics* (Konings, W. N., Kaback, H. R., and Lolkema, L. S., Eds.) Vol. 2, pp 137−163, Elsevier, Amsterdam.
7. Loe, D., Deeley, R. G., and Cole, S. P. C. (1996) *Eur. J. Cancer 32A*, 945−957.
8. Riordan, J. R., Rommens, J. M., Kerem, B., Alon, N., Rozmahel, R., Grzelczak, Z., Zielenski, J., Lok, S., Plavsic, N., Chou, J. L., et al. (1989) *Science 245*, 1066−1073.
9. Van Veen, H. W., Venema, K., Bolhuis, H., Oussenko, I., Kok, J., Poolman, B., Driessen, A. J., and Konings, W. N. (1996) *Proc. Natl. Acad. Sci. U.S.A. 93*, 10668−10672.
10. Hung, L. W., Wang, I. X., Nikaido, K., Liu, P. Q., Ames, G. F., and Kim, S. H. (1998) *Nature 396*, 703−707.
11. Shapiro, A. B., and Ling, V. (1995) *J. Bioenerg. Biomembr. 27*, 7−13.
12. Urbatsch, I. L., Al-Shawi, M. K., and Senior, A. E. (1994) *Biochemistry 33*, 7069−7076.
13. Sharom, F. J., Yu, X., Chu, J. W. K., and Doige, C. A. (1995) *Biochem. J. 308*, 381−390.
14. Loo, T. P., and Clarke, D. M. (1995) *J. Biol. Chem. 270*, 21449−21452.
15. Loo, T. W., and Clarke, D. M. (1995) *J. Biol. Chem. 270*, 22957−22961.
16. Urbatsch, I. L., Sankaran, B., Weber, J., and Senior, A. E. (1995) *J. Biol. Chem. 270*, 19383−19390.
17. Senior, A. E., Al-Shawi, M. K., and Urbatsch, I. L. (1995) *FEBS Lett. 377*, 285−289.
18. Azzaria, M., Schurr, E., and Gros, P. (1989) *Mol. Cell. Biol. 9*, 5289−5297.
19. Müller, M., Bakos, E., Welker, E., Váradi, A., Germann, U. A., Gottesman, M. M., Morse, B. S., Roninson, I. B., and Sarkadi, B. (1996) *J. Biol. Chem. 271*, 1877−1883.
20. Hrycyna, C. A., Ramachandra, M., Germann, U. A., Cheng, P. W., Pastan, I., and Gottesman, M. M. (1999) *Biochemistry 38*, 13887−13899.
21. Urbatsch, I. L., Beaudet, L., Carrier, I., and Gros, P. (1998) *Biochemistry 37*, 4592−4602.
22. Hyde, S. C., Emsley, P., Hartshorn, M. J., Mimmack, M. M., Gileadi, U., Pearce, S. R., Gallagher, M. P., Gill, D. R., Hubbard, R. E., and Higgins, C. F. (1990) *Nature 346*, 362−365.
23. Mimura, C. S., Holbrook, S. R., and Ames, G. F. (1991) *Proc. Natl. Acad. Sci. U.S.A. 88*, 84−88.
24. Nayak, S., and Bryant, F. R. (1999) *J. Biol. Chem. 274*, 25979−25982.
25. Nadanaciva, S., Weber, J., and Senior, A. E. (1999) *Biochemistry 38*, 7670−7677.
26. Story, R. M., and Steitz, T. (1992) *Nature 355*, 374−376.

27. Abrahams, J. P., Leslie, A. G. W., Lutter, R., and Walker, J. (1994) *Nature 340*, 621−628.
28. Weber, J., and Senior, A. E. (1997) *Biochim. Biophys. Acta 1319*, 19−58.
29. Yoshida, M., and Amano, T. (1995) *FEBS Lett. 359*, 1−5.
30. Rost, B., and Sander, C. (1993) *J. Mol. Biol. 232*, 584−599.
31. Sander, C. (1994) *Proteins 19*, 55−72.
32. Rost, B. (1996) *Methods Enzymol. 266*, 525−539.
33. Vogan, K. J., and Gros, P. (1997) *J. Biol. Chem. 272*, 28289−28295.
34. Beaudet, L., and Gros, P. (1995) *J. Biol. Chem. 270*, 17159−17170.
35. Geitz, R. D., and Schiestl, R. H. (1996) *Methods Mol. Cell. Biol. 55*, 123−125.
36. Raymond, M., Ruetz, S., Thomas, T. Y., and Gros, P. (1994) *Mol. Cell. Biol. 14*, 277−285.
37. Beaudet, L., Urbatsch, I. L., and Gros, P. (1998) *Biochemistry 37*, 9073−9082.
38. Lerner-Marmarosh, N., Gimi, K., Urbatsch, I. L., Gros, P., and Senior, A. E. (1999) *J. Biol. Chem. 274*, 34711−34718.
39. Van Veldhoven, P. P., and Mannaerts, G. P. (1987) *Anal. Biochem. 138*, 45−48.
40. Szabó, K., Welker, E., Bokos, E., Müller, M., Roninson, I., Váradi, A., and Sarkadi, B. (1998) *J. Biol. Chem. 273*, 10132−10138.
41. Goodno, C. C. (1982) *Methods Enzymol. 85*, 116−123.
42. Laemmli, U. K. (1970) *Nature 227*, 680−683.
43. Gros, P., Croop, J., and Housman, D. (1986) *Cell 47*, 371−380.
44. Bianchet, M. A., Young, H. K., Amzel, L. M., and Pederson, P. L. (1997) *J. Bioenerg. Biomembr. 29*, 503−524.
45. Urbatsch, I. L., Sankaran, B., Bhagat, S., and Senior, A. E. (1995) *J. Biol. Chem. 270*, 26956−26961.
46. Shyamala, V., Baichwal, V., Beall, E., and Ames, G. F. (1991) *J. Biol. Chem. 266*, 18714−18719.
47. Bliss, J. M., Garon, C. F., and Silver, R. P. (1996) *Glycobiology 6*, 445−452.
48. Stein, A., Hunke, S., and Schneider, E. (1997) *FEBS Lett. 413*, 211−214.
49. Mildvan, A. S. (1997) *Proteins: Struct., Funct., Genet. 29*, 401−416.
50. Julien, M., and Gros, P. (2000) *Biochemistry 39*, 4559−4568.
51. Nadanaciva, S., Weber, J., and Senior, A. E. (1999) *J. Biol. Chem. 274*, 7052−7058.

BI001128W